Enhanced yield into the radiative channel in Raman nuclear resonant forward scattering

1992 J. Phys.: Condens. Matter 4 2663

(http://iopscience.iop.org/0953-8984/4/10/028)

J. Phys.: Condens. Matter 4 (1992) 2663–2685. Printed in the UK

Enhanced yield into the radiative channel in Raman nuclear resonant forward scattering

Yu V Shvyd'ko and G V Smirnov
I V Kurchatov Institute of Atomic Energy, Moscow 123182, Russia

Received 5 June 1991, in final form 30 September 1991

Abstract. Nuclear resonant scattering of γ-radiation in the *forward direction* was studied in a vibrated target. Special attention was given to revealing the enhanced yield into the radiative channel of the nuclear reaction due to *coherent* scattering. The radiative channel in the resonance scattering of 14.4 keV γ-quanta by ^{57}Fe nuclei normally amounts to only 10.9%. The remaining part of the scattering goes into the conversion channel. The nuclear target used in the experiment (stainless steel enriched in ^{57}Fe nuclei) was completely opaque to the incident resonant γ-radiation with frequency ω_s. When the target started to vibrate with frequency $\Omega/2\pi = 23.79$ MHz, it remained opaque to the primary radiation, whereas intense secondary radiation at new frequencies emerged from the target in the forward direction. The $\omega_s + \Omega$ and $\omega_s - \Omega$ spectral components dominated in the emission spectrum and their total relative intensity reached $29.0 \pm 1.5\%$ of the incident γ-radiation intensity. It was shown theoretically that such an essential enlargement of the yield into the radiative channel of the nuclear reaction was possible owing to conditions of *coherent enhancement* of the radiative channel and *anomalously weak reasonance absorption*, which were provided by vibrating the target. The effect can be observed if the nuclei move in unison in the *coherence volume*. All experimental data were well fitted in the frame of the chosen theoretical model.

1. Introduction

As known, the role of the radiative channel is not significant in the nuclear resonance scattering of γ-quanta on low-lying levels. The internal conversion channel dominates in the decay of the intermediate state formed in the scattering process. However, the coherent partial width of the radiative channel can vary under certain conditions. Trammell first showed [1] that in Bragg scattering of a γ-quantum from a crystal the radiative channel is enhanced by the value

$$\Delta\Gamma_B = \Gamma_{coh} \frac{2\pi N_1}{(\kappa d)^2 \sin\theta_B} \tag{1}$$

owing to correlated action of nuclei in the scattering. Here Γ_{coh} is the coherent width of the decay into the radiative channel of an isolated nucleus; d is the distance between nuclei; $\kappa = 2\pi/\lambda$, λ is the radiation wavelength; θ_B is the Bragg angle; and N_1 is the number of reflecting planes. However, the given formula for enhancement is valid only if the crystal thickness dN_1 is less than the resonance absorption length d^3/σ_R [2]. Therefore, in the case of resonance scattering on low-lying levels, where cross-sections of resonance absorption σ_R are usually large, the enhancement cannot be a significant effect. The γ-beam is expected to be mainly converted into electrons in thick targets.

0953-8984/92/102663 + 23 $04.50

However, just for the case of interaction with a thick crystal Afanas'ev and Kagan showed that the suppression of incoherent channels (conversion channel in particular) is possible [3]. The authors have found that the superpositional state of γ-radiation is formed in a thick crystal in Bragg scattering. This state is described by the Bloch wave, in which the amplitude of nuclear excitation may vanish. In these circumstances the number of reflecting planes N_1 that take part in scattering increases drastically. Despite the increase of N_1, the conversion process is suppressed owing to vanishing excitation amplitudes. At the same time the radiative channel is enhanced owing to a coherent scattering mechanism (see discussion in section 4 of [4]). The coherent enhancement of the radiative channel is a major cause of build-up of the superpositional states of γ-radiation and of maintaining the radiative channel in multiple nuclear scattering of γ-quanta in a crystal. Thus, to direct a nuclear reaction into the radiative channel, both the enhancement of radiative decay and decreasing of nuclear excitation amplitude are necessary conditions. Reviews of theoretical and experimental work on this subject can be found in [5–7].

Now we shall turn to the possibility of change of a nuclear reaction yield in scattering of γ-quanta by irregular nuclear systems, for example in fine crystalline or amorphous targets. Afanas'ev and Kagan have shown in [2] that the enhancement of the radiative channel is accompanied by directed re-emission of γ-quanta not only in the Bragg direction but also in the forward direction. The waves scattered by nuclei in the foward direction have the same phase independently of nuclei position in the target space. Thus, it is obvious that, owing to the coherent nature of the forward scattering, the enhancement effect should exist in any nuclear target, including a target containing an irregular nuclear system. However, no visible enlargement of the yield into the radiative channel is seen in the conditions of usual resonant γ-quanta propagation through a nuclear target. The main effect observed is incoherent scattering, which removes γ-quanta from the primary beam. It occurs because of the destructive interference of primary and secondary radiation re-emitted in the forward direction. Obviously, in order to obtain a *coherently enhanced* re-emission of γ-quanta by nuclei, one must *exclude destructive interference* between incident and re-emitted radiation.

This can be done in different ways. Conceptually the most obvious way is to chop the incident radiation and to observe the secondary radiation re-emitted by nuclei in the forward direction [8]. The other possibility is to employ very short synchrotron radiation pulses for exciting a nuclear system [9]. In each case a spontaneous decay of prepared nuclear excitation occurs and coherent emission of γ-quanta in the forward direction takes place. The character of the interference between the primary and secondary waves can be changed by means of phase modulation of incident radiation [10–13]. In [12, 13] the phase was changed, for example, in a stepwise manner by displacement of a source towards a target for a half-wavelength distance. As a result of displacement, constructive rather than destructive interference of the waves arose in a target, and the detector recorded an intense flash of γ-radiation. In [14] the radiating nuclei were rapidly and synchronously transferred from one energy sublevel of the excited state to another. In this case the nuclear excitation decays mainly into the radiative channel, which is revealed in intense emission of radiation at changed frequency.

In the present paper nuclear forward scattering is studied under conditions where resonant γ-radiation interacts with the target subjected to ultrasonic excitation. Similar experiments were performed in [15–16]. However, in [15–16] the emphasis was on the modulation of γ-radiation, whereas in our study the emphasis is on the investigation of the enhancement of the radiative channel in the scattering reaction. For this purpose

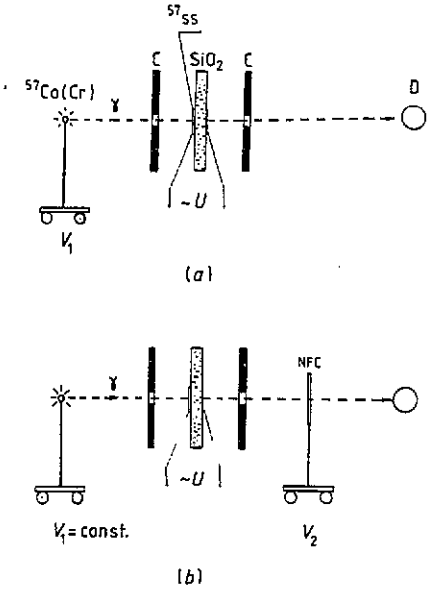

Figure 1. (*a*) Scheme of the experimental set-up for measuring absorption spectra in the vibrated ^{57}SS target. The target is stuck on a quartz piezocrystal, X-cut. Oscillation frequency is 23.79 MHz. The 14.4 keV γ-radiation source ^{57}Co(Cr) is moved in the constant-acceleration mode by the transducer V_1. (*b*) Scheme of the experimental set-up for measuring spectra of γ-radiation emerging from the vibrated ^{57}SS target in the forward direction. A single line resonance filter NFC, $K_2Mg[^{57}Fe(CN)_6].10H_2O$, is used for measuring the spectra by a transducer V_2. It is moved in constant-acceleration mode. The ^{57}Co(Cr) source on the transducer V_1 is moved in constant-velocity mode. C are collimators.

the target was made of a thickness that is very large in comparison with the absorption length. It was demonstrated that in such circumstances enhanced yield of a nuclear reaction into the radiative channel indeed takes place. The results of early experiments were published in [17].

Theoretical analysis has shown that the effect observed is caused not only by enhancement of radiative decay of nuclear excitations but also by a suppression of incoherent channels. The latter has an analogy with the Afanas'ev–Kagan suppression effect [3]. In both cases an anomalously transmitted wave field is built up in the nuclear system. A key point in the theory of Afanas'ev and Kagan [3] is the strict periodicity of the scatterers' location in space. In the given situation of an irregular nuclear system, however, of significance is the requirement of synchronism of periodic motion of nuclei in the *coherence volume*, $V_c \gg \lambda^3$. Superposition of eigen waves with different frequencies arises instead of coherent superposition of waves with different wavevectors. As a result, in some superpositional states the amplitude of excitation of nuclei, moved periodically in time, can be made arbitrarily small.

A specific form of periodic perturbation of nuclear states and the method of formation of the radiation field anomalously transmitted through a target may be different, generally speaking. For example, another possibility is to affect the nuclear spins by a radiofrequency magnetic field. But the general characteristic of the scattering process should be the coherent enhancement of the radiative channel.

2. The nuclear reaction yield in the resonance scattering of γ-quanta by nuclei in a vibrated target. The experiment

2.1. Resonance absorption in a nuclear target at rest

The reaction of resonance scattering of 14.4 keV γ-quanta by ^{57}Fe nuclei was studied. The internal conversion coefficient for the 14.4 keV transition from the first excited state

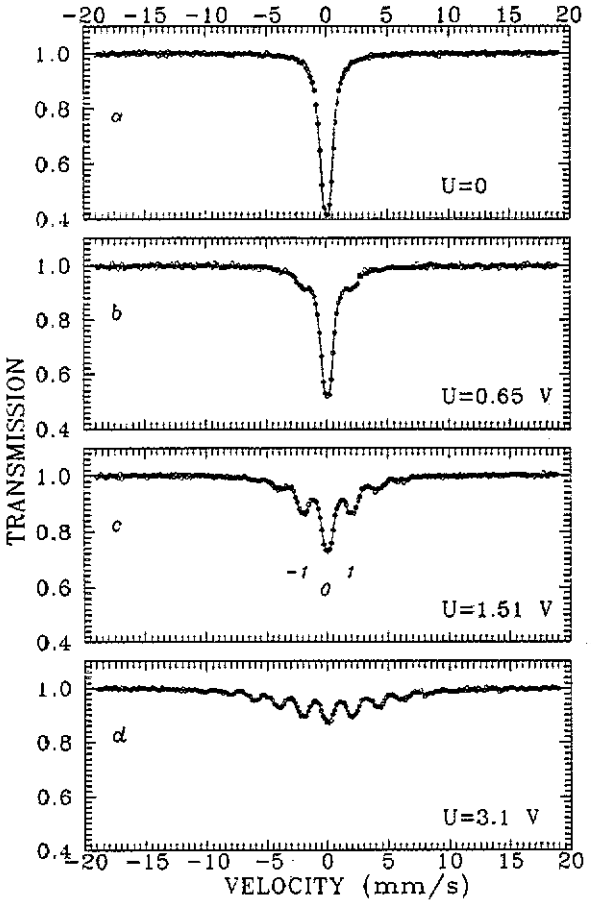

Figure 2. Absorption spectra of 14.4 keV Mössbauer radiation in the vibrated thick ^{57}ss target for various amplitudes U of driving voltage at the quartz plate.

equals 8.15. In other words, in scattering on isolated nuclei the γ-quanta are re-emitted in $R_{\text{lim}} = 10.9\%$ cases only. In all remaining cases conversion electrons are emitted. The nuclear target used in the experiment was opaque to the incident resonant γ-radiation.

The characteristics of γ-resonance absorption in the target were determined in the standard Mössbauer spectroscopy transmission scheme shown in figure 1(*a*). The ^{57}Co(Cr) source had an activity of 1.5×10^9 Bq and a linewidth $\Gamma_s = 0.15$ mm s^{-1}. It was driven into motion by the transducer V_1 which operated in the constant-acceleration mode. Stainless steel enriched by the resonance ^{57}Fe isotope up to 95% was used as the target (denoted ^{57}ss). It was manufactured as a foil of thickness $L = 12$ μm and diameter 6 mm (the weight of the foil was 2.4 ± 0.1 mg). The γ-beam illuminated only the central part of the target 6 mm in diameter. A detector with a crystal scintillator NaI(Tl), having area 0.8 cm^2, was used for recording γ-quanta. The detector was situated at a distance of 40 cm from the target. Therefore, it accepted γ-quanta that emerged from the target in a solid angle of not more than $\Delta = 5 \times 10^{-4}$ sterad about the forward direction.

The Mössbauer spectrum of the target is shown in figure 2(*a*). The absorption linewidth was equal to 1.25 mm s^{-1}, which is much greater than the nuclear γ-resonance

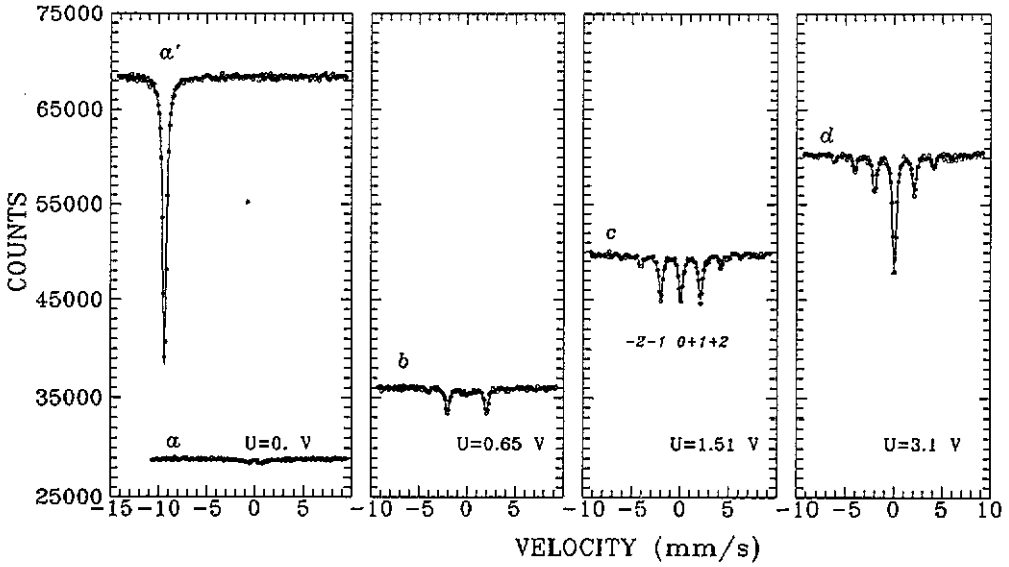

Figure 3. Spectra of γ-radiation emerging from the vibrated ^{57}ss target in the forward direction for various amplitudes U of driving voltage at the quartz plate. Measured by a single line resonance filter $K_2Mg[^{57}Fe(CN)_6].10H_2O$. The Mössbauer radiation from the ^{57}Co(Cr) source is tuned to the main absorption resonance (tagged by '0' in figure 2(*c*)). Full curves show results of the theoretical calculations (see section 4).

width in stainless steel†. Besides, the bottom of the resonance curve was rather flat. These results indicated that the resonance absorption of γ-quanta by nuclei reached saturation in the target under study.

The spectra shown in figures 3(*a*) and (*a'*) have another meaning. They represent the frequency distribution of γ-radiation emerging from the ^{57}ss target in the forward direction. Such spectra will henceforth often be called emission spectra. To measure emission spectra the resonance single line filter $K_2Mg[^{57}Fe(CN)_6].10H_2O$ was used. It was fixed on the transducer V_2—figure 1(*b*). The transducer operated in the constant-acceleration mode. The density of ^{57}Fe nuclei in the filter was 0.82 mg cm^{-2}, which corresponds to the resonance absorption factor $\mu_f l \simeq 11$. The spectrum in figure 3(*a'*) was measured in conditions when the source radiation line was shifted far from the resonance in ^{57}ss. This measurement made it possible to record the shape of the spectrum and to estimate the intensity of incident resonant γ-radiation with allowance for photo-electric absorption in the target. The dependence in figure 3(*a*) shows the spectrum of γ-quanta emerging from the ^{57}ss target in the case when the source line was in resonance with ^{57}Fe nuclei in ^{57}ss. As seen, in this case only a small part of incident γ-quanta left the target in the forward direction, namely the γ-quanta belonging to wings of the spectral distribution of the source. The intensity of transmitted quanta with respect to the incident radiation intensity (the spectrum in figure 3(*a'*)) amounted to 4.5 ± 1.0%‡

† The resonance width measured by conversion-electron Mössbauer spectrometry with the same source was 0.36 mm s^{-1}.

‡ All emission spectra in figures 3 and 5 are normalized at the same measurement time, namely 2 h. Therefore, to determine the intensity of any spectral line with respect to that of the source line (figure 3(*a'*)), the ratio of areas under these two curves was calculated.

only. Thus, 95.5 ± 1.0% of resonant γ-quanta striking the target was removed from the primary beam. This allows us to conclude that the target at rest was indeed a black absorber.

The conditions of the experiment were further changed.

2.2. Absorption spectra in conditions of ultrasonic excitation of the target

The nuclear target was driven into harmonic motion along the direction of γ-quanta propagation. For this purpose the ^{57}SS foil was stuck to an X-cut quartz piezocrystal slab 18 mm in diameter and 0.12 mm thick. The electrodes deposited on the plate were 6 mm in diameter. To excite the longitudinal vibrations in the quartz a sinusoidal electric voltage signal was supplied to the electrodes. The main resonance frequency of longitudinal vibrations of the piezocrystal with a stuck ^{57}SS foil was $\Omega/2\pi = 23.79$ MHz.

Figure 2 shows absorption spectra of resonance γ-radiation in the vibrated target. The measurements were carried out at different amplitudes U of the sinusoidal voltage applied to the piezocrystal slab and, hence, at different vibration amplitudes of the target. It is seen that, along with the main absorption line, a system of satellites has appeared in the spectrum, spaced apart at distances that are multiples of the oscillation frequency Ω. This result is well known from studies of the ultrasonic influence on Mössbauer spectra [18, 19]. However, an essential feature of the experiment under consideration is that a thick nuclear target is used here. It is this circumstance that causes a peculiarity of the results discussed below.

When the amplitude of the oscillations grows, the intensity of the central line in the absorption spectrum decreases. This implies that, whereas earlier the target was practically opaque for radiation tuned to resonance, now a noticeable part of the radiation ($\approx$50% at $U = 1.51$ V) emerges from the target in the forward direction. This single fact might not seem to be unusual. The action of thermal atomic motion is similar, for example. But in our case the increased transparency can no longer be simply attributed to resonance detuning due to vibrations, since enhanced transparency is observed without narrowing of the absorption line (see also section 3.3.4).

Let us discuss the results of studying the spectral distribution of radiation emerging from the target in the forward direction.

2.3. Spectra of γ-radiation emerging from the vibrated nuclear target

The spectral distribution of radiation leaving a vibrated target must depend on a particular resonance line excited in the absorption spectrum [18]. Let us first consider a symmetric situation, when the energy of the incident radiation is tuned to a central resonance in the vibrated ^{57}SS target. It is marked by '0' in figure 2(b).

2.3.1. Excitation of the main absorption resonance. The spectra of γ-radiation leaving the vibrated target in the forward direction (see figure 3) are characterized by some general features. Namely, the quasi-monochromatic source radiation with main frequency ω_s is transformed into polychromatic radiation with a set of spectral lines $\omega_s \pm \Omega k$ ($k = \pm 1, \pm 2, \ldots$) spaced apart at distances that are multiples of the oscillation frequency Ω. This phenomenon was observed for the first time by Asher *et al* [15] and later by Tsankov [16]. The lines in the spectra in figure 3 have a width that is very close to the source linewidth in figure 3(a').

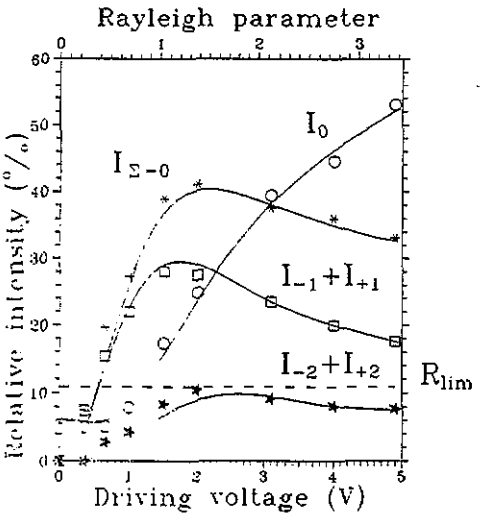

Figure 4. Relative intensities of spectral components of γ-radiation emerging in the forward direction from the vibrated ^{57}ss target for various amplitudes U of driving voltage at the quartz plate. The Mössbauer radiation from the ^{57}Co(Cr) source is tuned to the main absorption resonance (tagged by '0' in figure 2(*c*)). I_0 is the intensity of the central line in the emission spectra ('0' in figure 3(*c*)), which coincides in frequency with the ^{57}Co source radiation line; $I_{\Sigma-0}$ are all combinational lines except the central one; $I_{-1} + I_{+1}$ is the sum of intensities of combinational lines '−1' and '+1' (figure 3(*c*)); $I_{-2} + I_{+2}$ is the sum of intensities of combinational lines '−2' and '+2' (figure 3(*c*)). Full curves show results of the theoretical calculations (see section 4).

The presence of shifted lines in the measured spectra evidences that we are dealing here with secondary, inelastically scattered γ-radiation. The scattering process proceeds via the formation of an intermediate excited state of a nucleus and is accompanied by either absorption or emission of ultrasonic phonons—one, two or more. This is a kind of nuclear Raman scattering. The contribution of small-angle electronic scattering to the formation of the spectra was not detected in a test experiment. This means that the spectra observed are formed due to scattering on the nuclei only. Recall that the detector has recorded γ-quanta re-emitted by the target within a very small solid angle and in the forward direction only. The basic question we are interested in here is: What is the relative intensity of secondary radiation re-emitted in the forward direction?

It is seen from the spectrum in figure 3(*b*) that the nuclear target, driven into vibration with small amplitude $U = 0.65$ V, emits at combinational frequencies $\omega_s + \Omega$ and $\omega_s - \Omega$, whereas the line with the frequency of incident radiation ω_s is in fact absent. Such a result can obviously be obtained in a very thick nuclear target only†. The total intensity of two shifted lines $I_{+1} + I_{-1}$ amounts to $15.0 \pm 1.0\%$ of the incident radiation intensity. This implies that, even with a small driving voltage U, the radiative channel quota in the reaction of resonance scattering of γ-quanta on nuclei in the vibrated target exceeds the radiative channel quota $R_{lim} = 10.9\%$ on an isolated ^{57}Fe nucleus. As the driving voltage grows, the number and intensity of shifted lines increases. The central line with frequency ω_s appears here along with shifted ones. Note also that, as the vibration amplitude increases, the levels of intensity at infinite velocity in the spectra grow. This is due to increase of the total number of resonance quanta leaving the target in the forward direction.

Figure 4 shows the values of relative intensities of different spectral components in the emission spectra versus the driving voltage amplitude U. These data were obtained by processing a number of spectra. It is seen that the total relative intensity of shifted lines $I_{\Sigma-0}$ (without allowance for non-shifted component I_0 with frequency ω_s) reaches $40.5 \pm 1.5\%$. The most intense shifted lines are $\omega_s + \Omega$ and $\omega_s - \Omega$. Their total intensity

† The main frequency ω_s has always dominated in emission spectra described in the experiments [18, 19].

$I_{+1} + I_{-1}$ reaches $29.0 \pm 1.5\%$. The concentration of a substantial amount of secondary radiation in a small solid angle about the forward direction points to the *coherent* character of re-emission by the nuclei.

With due account of the fact that γ-quanta with shifted energy are products of decay of the intermediate excited state of the nuclei formed in the inelastic scattering reaction, we conclude that the effect of *enhanced yield* into the radiative channel in Raman nuclear forward scattering is observed.

Since the $40.5 \pm 1.5\%$ yield into the radiative channel was determined from shifted line intensities only, this yield value is a lower-limit estimate. As for the radiation at non-shifted frequency ω_s, it might appear at the target exit for at least two reasons. First, the radiation might pass through a vibrated target without interaction. Secondly, it might arise as a result of multiple Raman scattering. The experimental data available do not allow us to make any certain choice among these two possible mechanisms. However, the theoretical analysis done in section 3.2 (formula (3.23)) favours the multiple Raman scattering mechanism. Therefore, it is quite probable that the actual radiative channel yield is greater than the $40.5 \pm 1.5\%$ value given above.

The secondary radiation leaving the target has high intensity. For this situation to occur it is necessary, along with the *high probability of re-emission* into the radiative channel, to have the conditions of *anomalously weak resonance absorption* of radiation in traversing a thick target. The latter conclusion has an additional strong proof in the experiment described below.

2.3.2. Excitation of the first sideband resonance. Unlike the experiment described in the previous section, the primary γ-radiation was tuned to the first sideband resonance (marked by symbol '-1' in figure 2(c)) in the absorption spectrum of the target, i.e. $\omega_s = \omega_0 - \Omega$. Emission spectra obtained in these circumstances are shown in figure 5.

As in the previous case, the emission spectra consist of equidistant lines. However, this time the spectra are asymmetric (the asymmetry was also observed in [15]). As previously, the main attention will be given to the relative intensities of shifted lines. It is seen from figures 5(b)–(d) that the '$+1$' line in the emission spectra is the most intense one among all shifted ones. Its frequency $\omega_s + \Omega$ coincides with frequency ω_0 of the strongest absorption resonance in the ^{57}SS target. At the same time, the line '-1' with frequency $\omega_s - \Omega$, shifted far away from the main absorption resonance, is the less intense one. This result may seem rather surprising, since the nuclear medium should be a strong absorber at ω_0 or, in other words, it should be an incoherent scatterer. Instead of this, the system intensively emits radiation in the forward direction at the frequency of the main resonance, and the radiation with this frequency traverses the target with anomalously weak absorption. It occurs that some specific conditions arise in the vibrated target, due to which the nuclear resonance medium is converted from an incoherent scatterer of radiation into a coherent one.

Figure 6 presents the results of processing a number of emission spectra measured in these conditions. The intensities of shifted lines are given as a function of the driving voltage amplitude applied to the quartz slab. Note that the relative intensity of quanta emitted by a vibrated nuclear target into the '$+1$' frequency mode only reaches $I_{+1} = 15.0 \pm 1.0\%$. This means that re-emission even at one frequency that coincides with the frequency of the main absorption resonance in the target exceeds the radiative channel quota in the reaction of a γ-quantum resonance scattering on an isolated ^{57}Fe nucleus: $I_{+1} > R_{\text{lim}} = 10.9\%$.

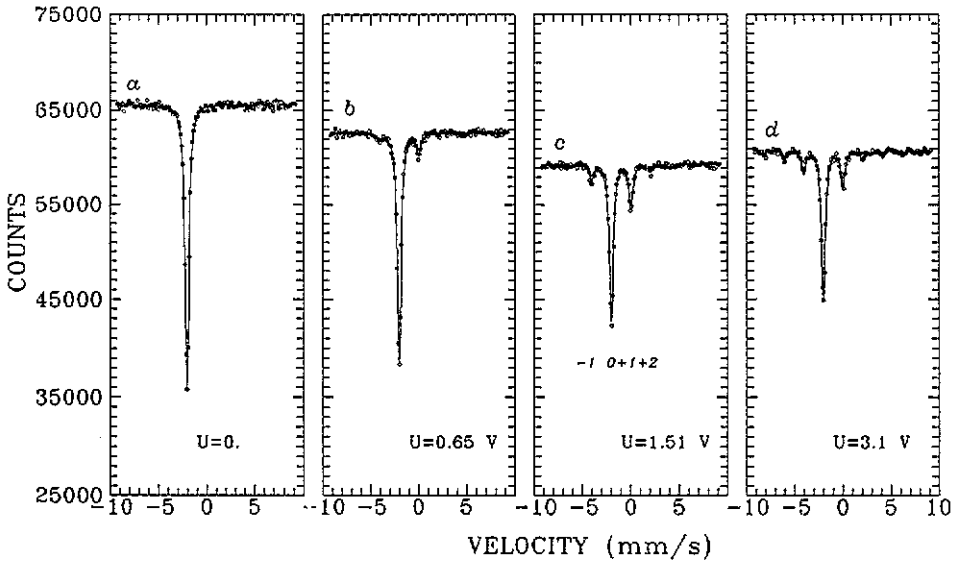

Figure 5. Spectra of γ-radiation emerging from the vibrated ^{57}ss target in the forward direction for various amplitudes U of driving voltage at the quartz plate. Measured by a single line resonance filter $K_2Mg[^{57}Fe(CN)_6].10H_2O$. The Mössbauer radiation from the ^{57}Co(Cr) source is tuned to the first sideband in the absorption spectrum (tagged by '-1' in figure 2(c)). Full curves show results of the theoretical calculations (see section 4).

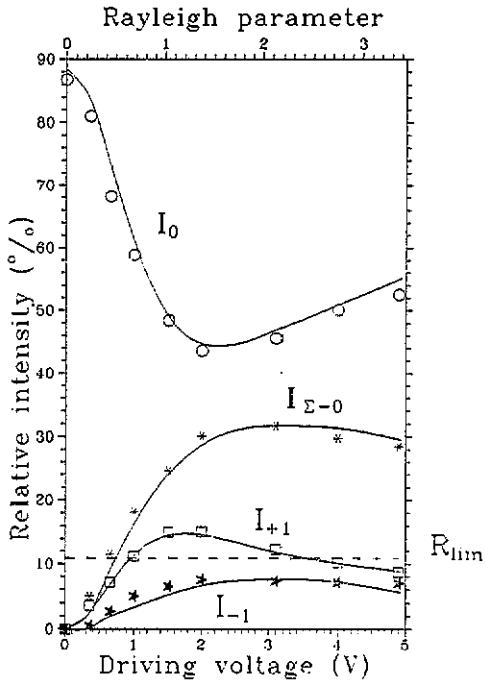

Figure 6. Relative intensities of spectral components of γ-radiation emerging in the forward direction from the vibrated ^{57}ss target for various amplitudes U of driving voltage at the quartz plate. The Mössbauer radiation from the ^{57}Co(Cr) source is tuned to the first sideband in the absorption spectrum (tagged by '-1' in figure 2(c)). I_0 is the intensity of the main line in the emission spectra ('0' in figure 5(c)), which coincides in frequency with the ^{57}Co source radiation line; $I_{\Sigma-0}$ are all combinational lines except the main one; I_{-1} and I_{+1} are intensities of combinational lines '-1' and '$+1$' (figure 5(c)), respectively. Full curves show results of the theoretical calculations (see section 4).

3. Interaction of γ-radiation with nuclei in the vibration target. Theory

The theoretical model that corresponds to the experiment is presented. Similar problems have been solved earlier in [20–22]. A particular feature of the solution technique used here is the direct description of the dynamics of formation of various spectral components of radiation in the course of multiple coherent Raman nuclear scattering of radiation in a vibrated target. The analysis of the solution obtained makes it possible to reveal immediately the radiative channel enhancement effect. The influence of synchronism of nuclei motion on the enhancement of a nuclear reaction yield into the radiative channel is considered.

3.1. The wave equation for radiation propagating in a vibrated resonance medium

The problem of propagation of a radiation wave $\mathscr{E}_\omega \exp[i(\kappa r - \omega t)]$ through a plane target of thickness L that contains spatially disordered resonance nuclei is solved. Here $\mathscr{E}_\omega$ is the amplitude of the wave with frequency ω and wavevector κ ($\kappa = 2\pi/\lambda$). The nuclei possess a low-lying isomeric level with energy $\hbar\omega_0$, close to $\hbar\omega$. The level width is $\Gamma = \Gamma_1 + \Gamma_2$, where Γ_1 and Γ_2 are partial widths of radiative and conversion decay channels, respectively. For low-lying excited states of nuclei the condition $\Gamma_2/\Gamma_1 \gg 1$ is valid as a rule. Therefore, in traversing the target at rest, the resonance radiation is mainly converted into electrons. The peculiarity of the problem of γ-resonance scattering under consideration is that the nuclei in the target are vibrated at ultrasonic frequency $\Omega/2\pi$.

Since the tangential component of the electric field intensity is continuous at the media interface, it can be presented inside a target as follows:

$$\boldsymbol{E}(\boldsymbol{r}, t) = \boldsymbol{E}_\omega(z, t) \exp[i(\kappa r - \omega t)]. \tag{3.1}$$

Here $\boldsymbol{E}_\omega(z, t)$ is the envelope of the electric field intensity; the z axis is perpendicular to the entrance surface of the target. In the linear-in-the-field approximation the current density $\boldsymbol{J}(\boldsymbol{r}, t)$ induced by incident radiation can be expressed in terms of its envelope $\boldsymbol{J}_\omega(z, t)$ by an equation similar to (3.1).

Since the amplitude of γ-radiation scattering on a separate nucleus is much less than λ and the frequency Ω of the target vibrations is much less than ω, the $\boldsymbol{E}_\omega(z, t)$ and $\boldsymbol{J}_\omega(z, t)$ envelopes are, obviously, slowly varying functions compared to the exponent in (3.1). To describe the radiation propagation in a medium the reduced version of the wave equation (see e.g. [23]) can be used in this case:

$$\gamma\, \partial \boldsymbol{E}_\omega / \partial z = -(2\pi/c)\boldsymbol{J}_\omega \tag{3.2}$$

$$\boldsymbol{E}_\omega(0, t) = \mathscr{E}_\omega. \tag{3.3}$$

The quantity $\gamma = \sin\theta$ in (3.2) is the sine of the angle θ between the direction of radiation incidence κ/κ and the target surface. Equation (3.3) is the boundary condition for the problem under consideration.

Let us calculate the current density induced by incident radiation in a vibrated resonance target. $\boldsymbol{J}(\boldsymbol{r}, t)$ must contain two components in the general case. One of them stems from the interaction with atomic shell electrons, the other one from the interaction with resonance nuclei. The interaction with electrons proceeds instantaneously, in fact. Therefore, the vibrations will not introduce any additional change of phases of the waves scattered by electrons in the forward direction. Proceeding from this, we shall take into

account in the calculations the nuclear current only. It can be represented as a sum of currents of individual nuclei. It is convenient to perform calculations in a momentum representation:

$$\boldsymbol{J}(\boldsymbol{r}, t) = \int \frac{\mathrm{d}\boldsymbol{k}}{(2\pi)^3} \exp(\mathrm{i}\boldsymbol{k}\cdot\boldsymbol{r}) \sum_a \exp(-\mathrm{i}\boldsymbol{k}\cdot\boldsymbol{r}_a) \langle a(t)|\, \hat{\boldsymbol{j}}(\boldsymbol{k}) |a(t)\rangle. \tag{3.4}$$

Here $\langle a(t)|$ is the wavefunction of the ath nucleus; $\hat{\boldsymbol{j}}(\boldsymbol{k})$ is the current density operator of a nucleus in $\boldsymbol{k}$-space; $\boldsymbol{r}_a$ is the radius vector of the ath nucleus. It is convenient to represent $\boldsymbol{r}_a$ as a sum: $\boldsymbol{r}_a = \boldsymbol{R}_a + \boldsymbol{u}_a(t)$, where $\boldsymbol{R}_a$ is the radius vector of the mean position of a nucleus and $\boldsymbol{u}_a(t)$ is the deviation from this position. The influence of thermal vibrations will be taken into consideration by introducing the Lamb–Mössbauer factor f_{LM} in final formulae. And, for the time being, we shall assume that $\boldsymbol{u}_a(t)$ describes the vibrations induced by an external source only.

The current density for the individual nucleus in the first non-vanishing order of the perturbation theory is equal to

$$\langle a(t)|\hat{\boldsymbol{j}}(\boldsymbol{k})|a(t)\rangle = -\mathrm{i} \exp[-\mathrm{i}(\omega_0 - \mathrm{i}\Gamma_0/2)t] \times \int_{-\infty}^{t} \mathrm{d}\tau \exp[\mathrm{i}(\omega_0 - \mathrm{i}\Gamma_0/2)\tau] \langle g|\hat{\boldsymbol{j}}(\boldsymbol{k})|e\rangle \langle e|\hat{V}_a(\tau)|g\rangle. \tag{3.5}$$

Here $\hat{V}_a$ is the Hamiltonian of interaction of the ath nucleus with the radiation field; $|e\rangle$ and $|g\rangle$ are wavefunctions of excited and ground states of a nucleus, which are $(2I_e + 1)$ and $(2I_g + 1)$ times degenerate respectively; I_e and I_g are nuclear spins in the excited and ground states. To calculate (3.5) the standard expression for $\hat{V}_a$ is employed:

$$\hat{V}_a(t) = -c^{-1} \int \mathrm{d}\boldsymbol{r}\, \hat{\boldsymbol{j}}(\boldsymbol{r} - \boldsymbol{r}_a) \boldsymbol{A}(\boldsymbol{r}, t). \tag{3.6}$$

If the Coulomb gauge condition is chosen, then in the slowly varying envelope approximation the vector potential $\boldsymbol{A}(\boldsymbol{r}, t)$ is expressed in terms of the electric field envelope as follows:

$$\boldsymbol{A}(\boldsymbol{r}, t) = -\mathrm{i}c\omega^{-1} \boldsymbol{E}_\omega(z, t) \exp[\mathrm{i}(\boldsymbol{\kappa}\boldsymbol{r} - \omega t)]. \tag{3.7}$$

Substituting (3.7) into (3.6), we obtain after simple transformations

$$\hat{V}_a(t) = \mathrm{i}\omega^{-1} \hat{\boldsymbol{j}}^*(\boldsymbol{\kappa}) \cdot \boldsymbol{E}_\omega(z_a, t) \exp[\mathrm{i}(\boldsymbol{\kappa}\boldsymbol{r}_a - \omega t)]. \tag{3.8}$$

In view of equations (3.5) and (3.8) the expression for the current density takes on the form:

$$J^s(\boldsymbol{r}, t) = \frac{f_{\mathrm{LM}}}{\omega(2I_g + 1)} \exp[-\mathrm{i}(\omega_0 - \mathrm{i}\Gamma_0/2)t] \int \frac{\mathrm{d}\boldsymbol{k}}{(2\pi)^3} \exp(\mathrm{i}\boldsymbol{k}\boldsymbol{r}) \times \sum_a \exp[\mathrm{i}(\boldsymbol{\kappa} - \boldsymbol{k})\boldsymbol{R}_a - \mathrm{i}\boldsymbol{k}\boldsymbol{u}_a(t)] \sum_{e,g} \langle g|\hat{j}^s(\boldsymbol{k})|e\rangle \langle e|\hat{j}^{s'*}(\boldsymbol{\kappa})|g\rangle \times \int_{-\infty}^{t} \mathrm{d}\tau\, E_\omega^{s'}(z_a, \tau) \exp[-\mathrm{i}(\omega - \omega_0 + \mathrm{i}\Gamma_0/2)\tau + \mathrm{i}\boldsymbol{\kappa}\boldsymbol{u}_a(\tau)]. \tag{3.9}$$

This formula includes the summation over all intermediate excited states $|e\rangle$ and averaging over initial states $|g\rangle$. Expression (3.9) takes into account the influence of thermal vibrations by introducing the factor f_{LM}. Index s $(s') = 0, 1$ labels components of orthogonal polarizations of the electric field.

We shall assume that longitudinal (along the normal $\boldsymbol{n}$ to the surface) vibrations of nuclei are excited in a nuclear target, as took place in the experiment:

$$u_a(t) = nd_a \sin(\Omega t + \varphi_a). \tag{3.10}$$

Suppose that nuclei vibrate in unison. This implies that $d_a = \text{const}$ and $\varphi_a = \text{const}$ throughout the target volume. In other words, the target is vibrated as a whole. Then the factor $\exp[ib_a \sin(\Omega t + \varphi_a)]$, where $b_a = (\boldsymbol{\kappa n})d_a$ is the modulation index, can be placed outside the summation sign. Since nuclei in the target are spatially disordered, the summation over the nuclei in (3.9) can be replaced by integration. As a result, the following explicit expression for the nuclear current density in a vibrated target is obtained:

$$J^s(\boldsymbol{r}, t) = J^s_\omega(z, t) \exp[\mathrm{i}(\boldsymbol{\kappa r} - \omega t)] \tag{3.11}$$

where the envelope is equal to

$$J^s_\omega(z, t) = -\frac{\omega\Gamma_0}{8\pi} g_0^{ss'} \exp[\mathrm{i}\alpha(t)] \int_{-\infty}^{t} \mathrm{d}\tau \exp[-\mathrm{i}\alpha(\tau)]\, E^{s'}_\omega(z, \tau) \tag{3.12}$$

with

$$\alpha(t) = (\omega - \omega_0 + \mathrm{i}\Gamma/2)t - b \sin(\Omega t + \varphi) \tag{3.13}$$

$$g_0^{ss'} = -\frac{8\pi N_0 f_{\mathrm{LM}}}{\omega^2(2I_g + 1)\Gamma_0} \sum_{e,g} \langle g|\hat{f}^s(\boldsymbol{\kappa})|e\rangle\langle e|\hat{f}^{s'*}(\boldsymbol{\kappa})|g\rangle. \tag{3.14}$$

Variable Γ is introduced instead of Γ_0 in (3.13) without explicit calculations. It describes possible homogeneous or inhomogeneous γ-resonance broadening in the target. The following relation $\Gamma \geqslant \Gamma_0$ is valid. In (3.14), N_0 is the number of resonance nuclei in a target volume unit. In the case of degenerate nuclear levels the quantity $g_0^{ss'}$ in (3.12) and (3.14) can be transformed into the following form (see e.g. [3]):

$$g_0^{ss'} = -g_0\delta^{ss'} \qquad g_0 = (4\pi N_0/\boldsymbol{\kappa}^3)(\Gamma_{\mathrm{coh}}/\Gamma_0) = \sigma_{\mathrm{R}} N_0/\boldsymbol{\kappa} \tag{3.15}$$

$$\Gamma_{\mathrm{coh}} = f_{\mathrm{LM}}[(2I_e + 1)/2(2I_g + 1)]\Gamma_1. \tag{3.16}$$

Here σ_{R} is the cross-section of resonance absorption by a nucleus; Γ_{coh} is the coherent part of the radiative channel Γ_1. Relation (3.15) allows us to use hereafter the scalar formulation of (3.2) with the current density envelope given by (3.12). Index s will be omitted.

In conclusion to this section, we shall make a comment regarding the applicability of expressions for the current density obtained. In transition from (3.9) to (3.11)–(3.14) the summation over nuclei in a macroscopically large target volume was performed. At the same time it is clear that there exists some minimal volume (called the *coherence volume* V_c henceforth) in which the summation procedure over nuclei does already lead to (3.11)–(3.14). The following estimate is valid: $V_c^{1/3} \gg \lambda$. Let us consider now a more general case, namely synchronism of nuclei vibrations is not conserved throughout the target volume. At first, assume that synchronism is conserved nevertheless in any chosen part of the target volume, equal to the coherence volume with centre at point $\boldsymbol{r}$. Then for current density $\boldsymbol{J}(\boldsymbol{r}, t)$ one obtains relations similar to (3.11)–(3.14), but with parameters b and φ explicitly dependent on $\boldsymbol{r}$. If, however, the nuclei in the coherence volume do not vibrate in unison, then the expression for the current density will be quite different (see section 3.3.4).

3.2. Emission by a vibrated nuclear target. Solution of the wave equation

The solution of the wave equation (3.2) with $J_\omega(z, t)$ defined by expression (3.12) will be sought as a superposition of monochromatic waves:

$$E_\omega(z, t) = \sum_{k=-\infty}^{+\infty} E_k(z, \omega) \exp(-i\Omega k t). \tag{3.17}$$

In this case the boundary condition (3.3) will be given by

$$E_k(0, \omega) = \mathcal{E}_\omega \delta_{k,0}. \tag{3.18}$$

Such a form of solution implies that, inside the target, the vibrated nuclei generate radiation that along with the main harmonic ω contains a coherent sum of combinational harmonics $\omega \pm \Omega k$ as well. In a sufficiently thick target one should expect dynamic transfer from each combinational mode to all others, and vice versa. As a result, the amplitudes $E_k(z, \omega)$ must depend on z, which is used explicitly in equation (3.17).

Let us substitute (3.17) into (3.2) and (3.12). We shall also make use of the well known relation:

$$\exp(ib \sin \phi) = \sum_{n=-\infty}^{\infty} J_n(b) \exp(in\phi)$$

where $J_n(b)$ are Bessel functions of the first kind. Then, we equate terms with the same frequencies in the left- and right-hand sides of (3.2). As a result, we obtain a system of dynamic equations for amplitudes of combinational harmonics $E_k(z, \omega)$:

$$\gamma \frac{\partial E_k}{\partial z} = \frac{i\kappa}{2} \sum_{n=-\infty}^{\infty} G_{kn} E_n \tag{3.19}$$

where

$$G_{kn} = \sum_{q=-\infty}^{+\infty} \exp(-ik\varphi) J_{k+q}(b) G_q(\omega) J_{n+q}(b) \exp(-in\varphi) \tag{3.20}$$

$$G_q(\omega) = -g_0(\Gamma_0/2)/(\omega - \omega_0 - \Omega q + i\Gamma/2). \tag{3.21}$$

Coefficients G_{kn} of the system of dynamic equations (3.19) determine the amplitude of transfer from the nth combinational mode to the kth one. The structure of (3.19) resembles the system of dynamic equations for Mössbauer or X-ray diffraction, when the Bragg conditions are exactly fulfilled. However, the diffraction system is a finite one. As a rule, it contains two or more equations for the amplitudes of waves propagating in the forward direction and at Bragg angles. Such a system can be solved exactly (see e.g. [3]). It is seen from the structure of coefficients G_{kn} that in the general case one cannot limit the number of equations as far as the system (3.19) is concerned. A system of infinite order must be solved. Let us try to find the solution by the iteration method. The condition at a boundary (3.18) is used as a zero approximation. Substituting it into the right-hand side of (3.19), one gets

$$E_k^{(1)}(z, \omega) = \mathcal{E}_\omega[\delta_{k,0} + (i\kappa z/2\gamma) G_{k0}]. \tag{3.22}$$

Then, equation (3.22) is used as the next approximation. This procedure is continued

up to infinity. As a result, the solution of (3.19) is obtained in the form of a series expansion:

$$E_k(z,\omega) = \mathcal{E}_\omega \left[\delta_{k,0} + \frac{i\kappa z}{2\gamma} G_{k0} + \left(\frac{i\kappa z}{2\gamma}\right)^2 \frac{1}{2!} G_{kn} G_{n0} + \left(\frac{i\kappa z}{2\gamma}\right)^3 \frac{1}{3!} G_{kn} G_{nm} G_{m0} + \ldots \right]. \tag{3.23}$$

Summation over repeated indices is supposed here.

The structure of (3.23) shows that the amplitude of the kth spectral mode of radiation with the frequency $\omega + \Omega\kappa$ at depth z is a result of a *multiple Raman resonance re-emission* of primary radiation with frequency ω into this mode. The scattering proceeds via all possible combinational modes and through all possible paths. The zero mode is not an exception and is the result of similar re-emission processes as well.

The series (3.23) can be summed up, if one makes use of the relation:

$$\sum_{q=-\infty}^{+\infty} J_{k+q}(b) J_q(b) = \delta_{k,0}. \tag{3.24}$$

Using it together with expression (3.20) for G_{kn}, the manifold sums in (3.23) can be reduced to one-fold ones:

$$\sum_n G_{kn} G_{n0} = \exp(-ik\varphi) \sum_q J_{k+q}(b) G_q^2(\omega) J_q(b) \tag{3.25}$$

$$\sum_{n,m} G_{kn} G_{nm} G_{m0} = \exp(-ik\varphi) \sum_q J_{k+q}(b) G_q^3(\omega) J_q(b) \tag{3.26}$$

etc. Substituting (3.24) and (3.20) as well as (3.25), (3.26), etc, into equation (3.23), the series can be summed up and the expression for the amplitude of the kth combinational mode can be reduced to

$$E_k(z,\omega) = \mathcal{E}_\omega \exp(-ik\varphi) \mathfrak{E}_k(z,\omega) \tag{3.27}$$

with

$$\mathfrak{E}_k(z,\omega) = \sum_q J_{k+q}(b) J_q(b) \exp\left(\frac{i\kappa z}{2\gamma} G_q(\omega)\right). \tag{3.28}$$

The solution (3.27)–(3.28) satisfies equation (3.19) and boundary conditions (3.18). Thus the vibrated crystal transforms an incident monochromatic wave into a coherent superposition of waves with different combinational frequencies. Using (3.17) and (3.27) we write down the expression for the electric field envelope at depth $z < L$:

$$E_\omega(z,t) = \mathcal{E}_\omega \sum_q E_\omega^q(z,t) \tag{3.29}$$

$$E_\omega^q(z,t) = J_q(b) S_q(b,t) \exp\left(\frac{i\kappa z}{2\gamma} G_q(\omega)\right) \tag{3.30}$$

where

$$S_q(b,t) = \sum_k J_{k+q}(b) \exp[-i(\Omega t + \varphi)k] = \exp[i(\Omega t + \varphi)q - ib \sin(\Omega t + \varphi)]. \tag{3.31}$$

Expressions (3.1), (3.17) and (3.27)–(3.31) completely solve the problem. They enable one to calculate the intensity of radiation leaving a vibrated target as a function of any of the parameters.

We are interested, first of all, in the spectrum of radiation $I(z, \tilde{\omega})$ at the target exit at $z = L$. For this purpose we calculate the Fourier image of $E(z, t)$ using formula (3.1) in scalar form together with (3.17), (3.27) and (3.28):

$$E_\omega(z, \tilde{\omega}) = \mathscr{E}_\omega \sum_k \exp(-ik\varphi)\delta(\tilde{\omega} - \omega - \Omega k)\mathfrak{E}_k(z, \omega). \tag{3.32}$$

To calculate the radiation spectrum expression (3.32) must be squared modulo. Besides, it must be averaged over the target vibration phase φ, since there is no correlation between the phase of the incident γ-radiation and the phase of the target vibrations. As a result we obtain

$$I(L, \tilde{\omega}) = \sum_k |\mathscr{E}_{\tilde{\omega}-\Omega k}\mathfrak{E}_k(L, \tilde{\omega} - \Omega k)|^2. \tag{3.33}$$

If the source spectrum $|\mathscr{E}_\omega|^2$ is assumed to have a Lorentzian form

$$|\mathscr{E}_\omega|^2(\Gamma_s/2\pi)/[(\omega - \omega_s)^2 + (\Gamma_s/2)^2] \tag{3.34}$$

then the spectrum of γ-radiation leaving the vibrating target is expressed as

$$I(L, \tilde{\omega}) = \sum_k I_k(L, \tilde{\omega}) = \frac{\Gamma_s}{2\pi}\sum_k \frac{|\mathfrak{E}_k(L, \tilde{\omega} - \Omega k)|^2}{(\omega_s + \Omega k - \tilde{\omega})^2 + (\Gamma_s/2)^2}. \tag{3.35}$$

3.3. Analysis of the theoretical solution

3.3.1. Absorption and emission by nuclei vibrating in unison. As follows from (3.29)–(3.31), the wave $\mathscr{E}_\omega \exp[i(\boldsymbol{\kappa r} - \omega t)]$ incident on a vibrated target excites within it with probability amplitudes $J_q(b)$ an infinite number of discrete superpositional states of radiation $S_q(b, t)$—equation (3.31) numbered by index q. Each state $S_q(b, t)$ is a coherent sum of waves with different combinational frequencies†. It represents an eigenstate of radiation in a vibrated nuclear target. The content of harmonics in each superpositional state is the same at any depth in the target. A complex refractive index corresponds to each individual superpositional state. Its part associated with the nuclear resonance scattering equals $G_q(\omega)/2 = \kappa^{-1}[\nu_q(\omega) + i\mu_q(\omega)]$. The real part $\nu_q(\omega)$ is equal, according to (3.21), to

$$\nu_q(\omega) = -\kappa g_0[(\omega - \omega_0 - \Omega q)\Gamma_0/2]/[(\omega - \omega_0 - \Omega q)^2 + (\Gamma/2)^2]. \tag{3.36}$$

It describes, as usual, the change of γ-radiation phase due to coherent scattering on nuclei in the forward direction. The imaginary part $\mu_q(\omega)$ is the absorption coefficient of the qth superpositional state in a vibrated target. It is equal to

$$\mu_q(\omega) = \kappa g_0\,(\Gamma\Gamma_0/4)/[(\omega - \omega_0 - \Omega q)^2 + (\Gamma/2)^2]. \tag{3.37}$$

The nuclear absorption coefficient in a target at rest coincides with $\mu_0(\omega)$. Without loss of generality we shall suppose hereafter for simplicity that the frequency ω of incident radiation is close to the resonance frequency ω_0: $|\omega - \omega_0| \leqslant \Gamma$. Suppose also that the target is so thick that $\mu_0(\omega)L \gg 1$, or

$$\kappa g_0 L \gg 1. \tag{3.38}$$

With such a target thickness, the resonant radiation does not pass through the target at

† This gives rise, in particular, to the complex periodic time dependence of radiation intensity leaving the target—the so-called Perlow quantum beat effect [10, 11].

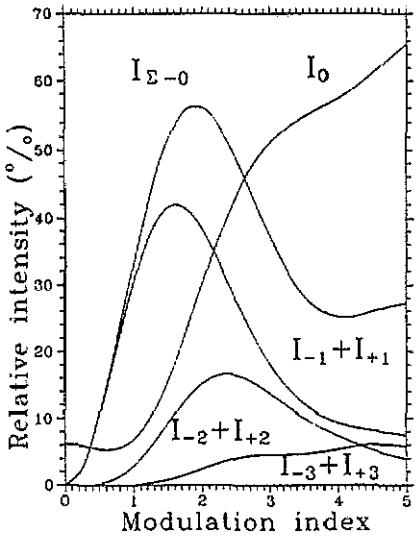

Figure 7. Relative intensities of spectral components of γ-radiation emerging in the forward direction from a vibrated nuclear target for various values of modulation index. Theoretical calculations are carried out in the frame of the model where the nuclei are moved in unison. The γ-radiation source is tuned to the main absorption resonance. Notations are similar to those used in figure 4.

rest. On the other hand, in the vibrated target, as follows from (3.36), for any thickness L, including that satisfying equation (3.38), one can find a number of superpositional states $\tilde{q}$ for which the opposite relation $\mu_q(\omega)L \ll 1$ is valid. This implies that radiation in the superpositional states, beginning with the $\tilde{q}$th one, will leave the target in the forward direction. The estimate for $\tilde{q}$ can be obtained from (3.37):

$$|\tilde{q}| \gg (\Gamma/2\Omega)(\kappa g_0 L)^{1/2}. \tag{3.39}$$

If the target vibration frequency is so large that the relation

$$\Omega \gg (\Gamma/2)(\kappa g_0 L)^{1/2} \tag{3.40}$$

is satisfied, then the radiation in all superpositional states, except for the zero one with $q = 0$, traverses through the target with anomalously low absorption. A similar conclusion was made earlier by Dzyublik [21]. One should note an important peculiarity here. For $\Omega \gg \Gamma/2$ the equality $\nu_q(\omega) \simeq (2\Omega q/\Gamma)\mu_q(\omega)$ is valid. This implies that, even if the condition of anomalous transmission is met, $\mu_q(\omega)L \ll 1$, the value of $\nu_q(\omega)L$ can be of the order of unity. In other words, the phase of the transmitted wave may differ greatly from the phase of the incident wave, and this evidences that the radiation passing through the target with anomalously low absorption is *secondary radiation*—the one that has experienced *interaction* with the nuclear system.

Let us see how the intensity of radiation leaving the target is shared among various spectral components. As mentioned above, all superpositional states contribute to each component. Figure 7 shows the values I_0, $I_k + I_{-k}$ $(k = 1, 2, 3)$ and $I_{\Sigma-0}$ as a function of modulation index b. The intensities of spectral components were determined as $I_k = \int d\bar{\omega}\, I_k(L, \bar{\omega})$ and calculated by formula (3.35). The parameters of the γ-radiation source and target applied in the experiment were used in the calculations (see section 4). At small vibration amplitudes ($b \leqslant 2$) the shifted spectral components are dominant in the spectrum. Their intensity amounts to $I_{\Sigma-0} = 56\%$ at $b = 1.9$. The lines with $k = \pm 1$ are the most intense ones. The total intensity of all spectral components, including the non-shifted one, reaches 92% at $b = 2.5$. Recall that the theoretical calculations were carried out in the frame of the model with nuclei moving in unison.

The dependences in figure 7 are in qualitative agreement with the experimental data given in figure 4. The quantitative correspondence between the theory and experiment is discussed in section 4.

The calculations have shown that resonance γ-quanta absorption and scattering in a vibrated nuclear target proceed in some unusual way. The target absorbs a considerable part of the radiation at frequency ω and re-emits it at frequencies $\omega \pm \Omega k$ ($k = 0, \pm 1, \pm 2, \ldots$). Besides, it is seen that the secondary radiation traverses the target with anomalous absorption. The nuclear reaction yield is obviously changed in favour of a radiative channel. Let us reveal the reasons for these phenomena.

3.3.2. Coherent enhancement of the radiative channel. The tendency to enhancement can be followed more easily in a thin target, $L < (\sigma_R N_0)^{-1}$, in which the resonance absorption has not yet reached saturation, i.e. when the effect is still dependent on the number of nuclei participating in the interaction. Let us calculate the amplitude of radiation re-emitted into the kth ($k \neq 0$) combinational mode. For this purpose we make use of equation (3.23). In so doing we shall consider one- and two-fold re-emission processes only, i.e.

$$E_k(L, \omega) \simeq \mathscr{E}_\omega[(i\kappa L/2\gamma)G_{k0} + (i\kappa L/2\gamma)^2(1/2!)G_{kn}G_{n0}]. \tag{3.41}$$

In view of equations (3.20), (3.21), (3.25), (3.15) and (3.16) and after some simple transformations, equation (3.41) can be presented in the form:

$$E_k(L, \omega) \simeq \mathscr{E}_\omega(i\kappa L/2\gamma)\tilde{G}_{k0} \tag{3.42}$$

where $\tilde{G}_{k0}$ is defined by (3.20)–(3.21) but with $G_q(\omega)$ changed therein to

$$\tilde{G}_q(\omega) = -g_0(\Gamma_0/2)[\omega - \omega_0 - \Omega q + i(\Gamma + \Delta\Gamma_0)/2]^{-1} \tag{3.43}$$

$$\Delta\Gamma_0 = \Gamma_{coh}\pi N_0 L/(\kappa^2 \sin\theta). \tag{3.44}$$

Equation (3.42) shows that the scattering process can effectively be treated as a result of a one-fold, rather than two-fold, Raman scattering act. Besides the resonance width of coherent scattering is increased by the value of $\Delta\Gamma_0$, which is seen explicitly from equations (3.43)–(3.44). The increase of the width is a direct manifestation of the enhancement effect of the radiative channel. Thus, the effect acts not only in a regular system of nuclei in the Bragg scattering, as was discussed in [1, 3], but also in irregular systems. However, in the case of coherent forward scattering, the width increases by the value of $\Delta\Gamma_0$ (3.44), which is exactly twice as low as the increase $\Delta\Gamma_B$ (1.1) that is reached in the Bragg scattering case. This difference can be attributed to the fact that in the Bragg case the re-emission can proceed in both the forward direction and at the Bragg angle [24], whereas an irregular nuclear system can re-emit coherently in the forward direction only.

From equations (3.42)–(3.44) one can find that the intensity of re-emission into the shifted spectral mode of the kth order is proportional to the square of the total number N of nuclei participating in the interaction:

$$I_k(L, \omega) \sim N^2. \tag{3.45}$$

The intensity of nuclear decay into the non-coherent channels, including the internal conversion one, is proportional to the first power of N. Thus, owing to coherent scattering, the role of the radiative channel increases. However, the enhancement might

be observed only if coherently re-emitted radiation survived in traversing the absorbing medium. Such conditions really do exist in the vibrated target.

3.3.3. The probability of nucleus excitation in a vibrated target. Let us estimate the probability to find a nucleus in the excited state, provided that it is located in a vibrated target. Similarly to the procedure of derivation of equation (3.5), one can show that the probability amplitude in the first non-vanishing order of the perturbation theory equals

$$\langle e|a(t)\rangle = -\mathrm{i}\exp[-\mathrm{i}(\omega_0 - \mathrm{i}\Gamma_0/2)t]\int_{-\infty}^{t} \mathrm{d}\tau \exp[\mathrm{i}(\omega_0 - \mathrm{i}\Gamma_0/2)\tau]\langle e|\hat{V}_a(\tau)|g\rangle \tag{3.46}$$

where index a indicates a nucleus located at depth z in the target. Since $E_\omega(z, t)$ is a sum of fields $E^q_\omega(z, t)$ ((3.29)–(3.30)) corresponding to different eigenstates of radiation, it is convenient to calculate the probability amplitude of a nucleus excitation for each eigenstate separately: $\langle e|a(t)\rangle_q$. Substituting (3.29) into (3.8) and further into (3.46), one obtains

$$\langle e|a(t)\rangle_q = \mathrm{i}\omega^{-1}\mathscr{C}_\omega\langle e|\hat{\jmath}^*(\boldsymbol{\kappa})|g\rangle\exp[\mathrm{i}\boldsymbol{\kappa}\boldsymbol{R}_a + (\mathrm{i}\kappa z/2\gamma)G_q(\omega)]$$
$$\times J_q(b)\exp[\mathrm{i}(\Omega t + \varphi)q]/(\omega - \omega_0 - \Omega q + \mathrm{i}\Gamma/2). \tag{3.47}$$

We will introduce the notation $W_0 = \langle e|a(t)\rangle_0/J_0(b)$. It follows from the definition that W_0 equals the excitation amplitude of a nucleus in a target at rest, i.e. under normal conditions. When (3.38) and (3.39) are satisfied, the ratio of the probability of a nucleus excitation by radiation in superpositional state with $q > \tilde{q}$ to the normal probability of a nucleus excitation W_0^2 is equal to

$$|\langle e|a(t)\rangle_q/W_0|^2_{z_a=0} \simeq J_q^2(b)(\Gamma/2\Omega q)^2 \tag{3.48}$$

and can be made arbitrarily small. Therefore, the radiation in these states traverses the target practically without losses into incoherent channels. This produces conditions for observation of the enhanced yield into the radiative channel.

3.3.4. Absorption and emission by nuclei vibrated in dissonance. So far we have considered the cases of resonance interaction of γ-radiation with nuclei moved in unison. In order to determine the role of synchronism in the enhancement effect, we shall consider in this section another limiting case—the interaction with nuclei moving in complete dissonance.

Let the nuclei be vibrated according to equation (3.10), but with different phases φ_a. The phases φ_a can take on any values from 0 to 2π with equal probability, i.e. there is no correlation of vibrations. In this case one cannot use (3.12) for current density in the right-hand side of the wave equation (3.2). To calculate the coherent component of the nuclear current density in these conditions, equations (3.9)–(3.10) must be averaged over φ_a. As a result, instead of (3.12)–(3.14) we obtain

$$J_\omega(z, t) = \frac{\omega\Gamma_0}{8\pi}g_0\sum_k J_k^2(b)\exp(\mathrm{i}\tilde{\omega}_k t)\int_{-\infty}^{t}\mathrm{d}\tau\exp(-\mathrm{i}\tilde{\omega}_k t)E_\omega(z, \tau)$$
$$\tilde{\omega}_k = \omega - \omega_0 - \Omega k + \mathrm{i}\Gamma_0/2. \tag{3.49}$$

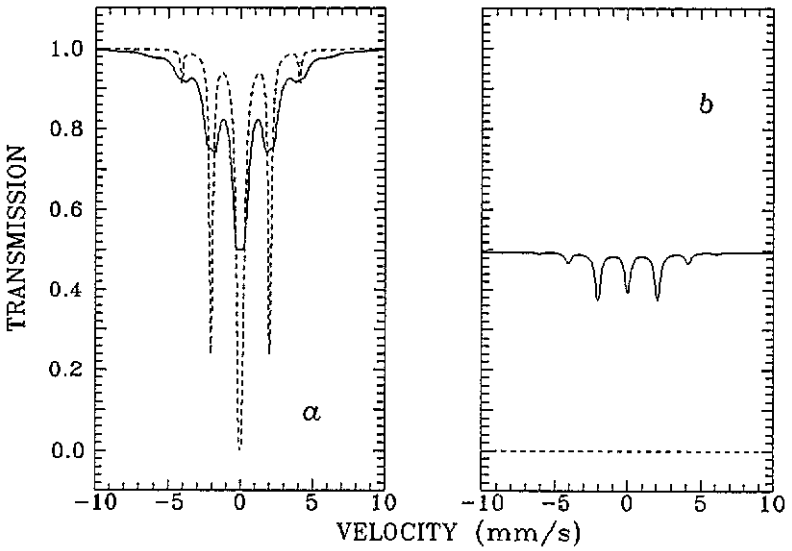

Figure 8. (*a*) Absorption spectra calculated for the case of synchronous (full curve) and non-synchronous (broken curve) vibrations of nuclei in a target. (*b*) Emission spectra calculated in similar conditions of synchronous and non-synchronous motion of nuclei. The incident radiation is assumed to be monochromatic. The nuclear resonance parameters are the same as in the experiment (see section 4). The distribution of vibration amplitudes given by equation (4.4) with $b_R = 1$ is taken into account. Bessel functions are averaged over the distribution.

The solution of wave equation (3.2) with current density expressed by (3.49) gives a result completely different from that given by (3.29)–(3.30).

$$E_\omega(z, t) = \mathscr{E}_\omega \exp\left(\frac{i\kappa z}{2\gamma} \sum_m J_m^2(b) G_m(\omega)\right). \tag{3.50}$$

One can see that in this case coherent re-emission in the forward direction proceeds at the *non-shifted frequency* only. Thus, if the vibrations of nuclei are not correlated, there are no conditions for coherent Raman scattering.

As seen from (3.50), there should be satellites in the absorption spectrum at frequencies $\omega_0 \pm \Omega m$ ($m = \pm 1, \pm 2, \ldots$) along with the main resonance at ω_0. Non-synchronous vibrations of nuclei influence the nuclear resonance interaction with radiation like the thermal oscillations do. The probability of recoilless absorption f_{LM} in the main resonance is decreased by a factor of $J_0^2(b)$. This in fact leads to resonance demolition. As for the rest, equation (3.50) is standard. Thus no conditions for enhanced yield into the radiative channel arise.

Figure 8(*a*) presents the example of comparison of absorption spectra and figure 8(*b*) of emission spectra in the synchronous (full curve) and non-synchronous (broken curve) motion modes at the same amplitudes of nuclear vibrations. As seen, the spectra are drastically different for these two vibrational modes. Let us consider the main resonance line in figure 8(*a*). In conditions of non-synchronous motion it drops down to the zero intensity level and is narrow. Meanwhile in conditions of synchronous motion it is not deep but wide (the width much more than Γ_0). In the first case no radiation at all could pass through the target when the frequency of the incident wave is tuned at resonance

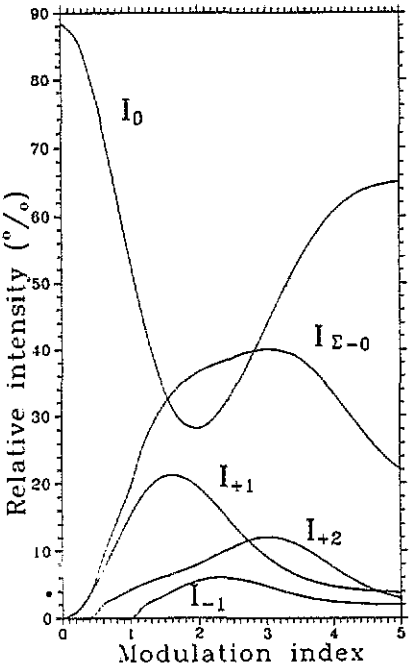

Figure 9. Relative intensities of spectral components of γ-radiation emerging in the forward direction from a vibrated nuclear target for various values of modulation index. Theoretical calculations are carried out in the frame of the model where nuclei are moved in unison. The γ-radiation source is tuned to the first sideband in the absorption spectrum. Notations are similar to those used in figure 6.

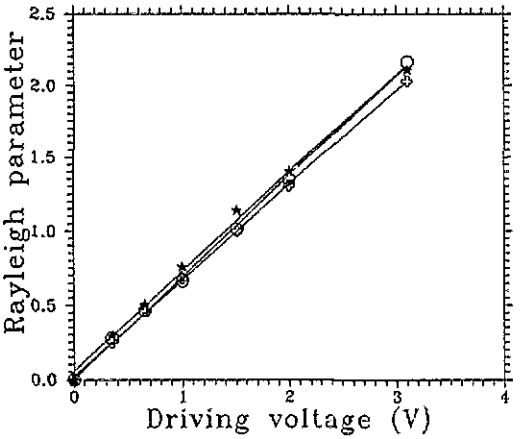

Figure 10. Correspondence between driving voltage amplitudes U and Rayleigh parameters b_R obtained from the fitting: (*a*) of the experimental absorption spectra (figure 2)—the b_R values are labelled by (+); (*b*) of the emission spectra (figure 3) at the excitation of the main resonance (*); (*c*) of the emission spectra (figure 4) at the excitation of the first absorption sideband (○).

(see also corresponding emission spectrum—lower curve in figure 8(*b*)). However, in the second case, as we discussed earlier, secondary radiation with a complicated spectrum is coherently emitted in the forward direction (upper curve in figure 8(*b*)).

The comparison accomplished shows that a reason such as demolition of the resonance due to vibrations of nuclei cannot be the reason for the appearance of intense radiation behind the nuclear target in the experiment described.

3.3.5. An example of qualitative discrepancy between the theory and experiment. Before making a quantitative comparison of the theory with the experiment, we shall present one more result of the calculations; namely, the calculation of intensities of lines in the emission spectra, when the first sideband resonance in a nuclear target is excited. The results of measurements carried out in these conditions were described in section 2.4.2. The results of calculations are presented in figure 9. They are valid for the case of synchronous motion of nuclei in the target. Comparing these results with the experimental data (figure 6), one can notice not only quantitative but also qualitative discrepancies. Both in the theory and in the experiment the line '+1' was the most intense one among all shifted lines. The line '−1' was found to be the next most intense one in the experiment, whereas according to the theory the line '+2' should be the next most

intense one. As will be shown in the following section, the quantitative and qualitative discrepancies can be eliminated by introducing in the model a partially non-synchronous motion mode of nuclei.

4. Comparison of the theory with experiment

So far we have mainly considered theoretically the case when nuclei were moving in unison. Another limiting case—the interaction with nuclei moving in complete dissonance—was considered in section 3.3.4. As we were convinced, the synchronism of nuclei vibrations in a target is an essential requirement for observing the enhancement effect. The experimental data of section 2 proved that this phenomenon was actually observed. At the same time, the data indicate that the effect was observed in the absence of full synchronism of nuclei motion in the target. This is seen already from the absorption spectra (figure 2). In the case of synchronous motion the relation of sideband intensities should be different, see e.g. [25]. Besides, as noted in section 3.3.5, the relation of the intensities of lines '+2' and '−1' in the experimental emission spectra (figures 5 and 6) is inverse to that obtained in the frame of the model of perfect synchronous motion. Perhaps the case of partial synchronism took place in the experiment.

Synchronism can be violated at both microscopic and macroscopic scales. In the second case, vibrations proceed synchronously within separate volumes, which are not smaller than V_c, but the motion of these volumes is not correlated. The wavelength of sound in SS at frequency $\Omega/2\pi = 23.79$ MHz equals $\Lambda = 210\ \mu$m, which is much larger than the γ-radiation wavelength $\lambda = 0.86$ Å. Hence, it is very likely that the non-synchronism of vibrations is macroscopic in these conditions.

As has already been noted at the end of section 3.1, the current density can be described in this case by equations (3.11)–(3.14), but with parameters b and φ being explicit functions of $\boldsymbol{r}$. As the target thickness $L = 10\ \mu$m is much less than Λ, it is natural to assume that this dependence includes x and y coordinates only. This means that the synchronism of nuclei vibrations is conserved in regions of cylindrical shape with area greater than $V_c^{2/3}$ and oriented perpendicular to the target surface. In this case we obtain for the γ-radiation field the solution of (3.27)–(3.32) type, as in the case of synchronous motion. However, the radiation spectrum (3.35) must be averaged over nuclei vibration amplitudes (the phases of vibrations φ do not appear in equation (3.35)):

$$I(L, \tilde{\omega}) = \sum_k I_k(L, \tilde{\omega}) = \frac{\Gamma_s}{2\pi} \sum_k \frac{\langle |\mathfrak{E}_k(L, \tilde{\omega} - \Omega k)|^2 \rangle}{(\omega_s + \Omega k - \tilde{\omega})^2 + (\Gamma_s/2)^2} \tag{4.1}$$

where

$$\langle |\mathfrak{E}_k(L, \tilde{\omega} - \Omega k)|^2 \rangle = \int_0^\infty \mathrm{d}b\, P(b) |\mathfrak{E}_k(L, \tilde{\omega} - \Omega k)|^2. \tag{4.2}$$

Here $P(b)$ is the distribution of modulation indices, which is associated with different vibration amplitudes of nuclei in the target.

Obviously, the averaging operation in (4.1)–(4.2) does not influence in any way the values of absorption factors $\mu_q(\omega)$ (3.37) for various superpositional states. Only the relations of intensities I_k of different spectral components change.

The emission spectra in figures 3 and 5 have been measured by means of a resonance single line filter. Therefore, they should be compared with (4.1)–(4.2) dependences convoluted with the spectral function of a resonance filter:

$$S_e(\omega_f) = \int d\bar{\omega}\, I(L, \bar{\omega}) \exp\left(-\frac{\mu_f l(\Gamma_0/2)^2}{(\bar{\omega} - \omega_f)^2 + (\Gamma_0/2)^2}\right) \qquad (4.3)$$

$$\omega_f = \omega_{f0}(1 - v_f/c).$$

Here ω_{f0} is the resonance frequency of the filter at rest; v_f is the velocity of the filter moved along the γ-beam propagation; c is the speed of light.

Good results of fitting the Mössbauer absorption spectra (figure 2) and emission spectra (figures 3–6) were obtained using the Rayleigh distribution for a modulation index:

$$P_R(b) = (b/b_R^2)\exp(-b^2/2b_R^2) \qquad (4.4)$$

with parameter b_R proportional to the characteristic vibration amplitude. It was the only free parameter in the fitting. The remaining parameters have been determined earlier from the procedure of fitting the experimental spectra (figure 2(a) and figure 3(a) and (a')) measured in the target at rest. The following parameters have been used. The nuclear resonance absorption factor in the target is $\kappa g_0 L = 90 \pm 3$; the resonance linewidth in a target with due account of inhomogeneous broadening is $\Gamma = (1.9 \pm 0.1)\Gamma_0$, where $\Gamma_0 = 0.097$ mm s^{-1}; the γ-radiation source linewidth is $\Gamma_s = (1.5 \pm 0.1)\Gamma_0$; the resonance absorption factor of the filter is $\mu_f l = 11 \pm 1$; the target vibration frequency is $\Omega/2\pi = 23.79$ MHz.

Figure 10 illustrates the correspondence between the amplitudes of driving voltage U at the quartz plate and the Rayleigh parameters b_R obtained from fitting the absorption spectra (figure 2) and emission spectra (figures 3 and 5). As seen, the spectra of various types, measured for the same values of voltage U, are well described by very close values of the Rayleigh parameter. Besides, the $b_R(U)$ dependences are linear to good accuracy in all three cases studied. The averaged dependence is $b_R = 0.69U$. The upper scales in figures 4 and 6 correspond to this calibration.

Thus, the model, which takes into account the amplitude inhomogeneity of nuclei vibrations, describe well all qualitative and quantitative features of experimental spectra.

5. Conclusions

The quasimonochromatic Mössbauer radiation was trapped almost completely by nuclei in a thick target vibrated along the γ-beam at ultrasonic frequency $\Omega/2\pi$ and then re-emitted in the forward direction at frequencies $\omega_s \pm \Omega k$, $k = 0, \pm 1, \pm 2, \ldots$ (ω_s is the primary radiation frequency). It turned out that in this case the fraction of the radiative channel in the reaction of γ-resonance scattering on nuclei has grown noticeably. The enhancement of the reaction yield into the radiative channel is achieved due to Raman coherent scattering of γ-quanta on nuclei in a vibrated target. A large part of the secondary radiation is weakly absorbed by a nuclear target even in the case when the energy of re-emitted quanta coincides with the main nuclear absorption resonance.

The theoretical approach used in this paper can be considered as a supplementary one to previously developed ultrasonic modulation theories [20–22]. The peculiar feature of

the present approach is the possibility to follow the mechanism of formation of γ-radiation states in a target due to multiple Raman coherent scattering on vibrated nuclei. It is also shown that to observe the radiative channel enhancement the condition of synchronous motion of nuclei in the target must be fulfilled at least in volumes not smaller than the coherence volume. The coherence volume is estimated by $V_c^{1/3} \gg \lambda$ (λ is the γ-radiation wavelength).

One should note that the method of coherent Raman scattering in thick nuclear targets can be efficiently utilized for frequency transformation of γ-radiation.

References

[1] Trammell G T 1961 *Chemical Effects of Nuclear Transformations* vol 1 (Vienna: IAEA) p 75
[2] Afanas'ev A M and Kagan Yu 1965 *Pis. Zh. Eksp. Teor. Fiz.* 2 130 (Engl. Transl. 1965 *JETP Lett.* 2 81)
[3] Afanas'ev A M and Kagan Yu 1965 *Zh. Eksp. Teor. Fiz.* **48** 327 (Engl. Transl. 1965 *Sov. Phys.–JETP* **21** 215)
[4] Maurus H J, van Bürck U, Smirnov G V and Mössbauer R L 1984 *J. Phys. C: Solid State Phys.* **17** 1991
[5] Kagan Yu and Afanas'ev A M 1972 *Mössbauer Spectroscopy and its Applications* (Vienna: IAEA) p 143
[6] Smirnov G V 1986 *Hyperfine Interact.* **27** 203
[7] van Bürck U 1986 *Hyperfine Interact.* **27** 219
[8] Shvyd'ko Yu V, Smirnov G V, Popov S L and Hertrich T 1991 *Pis. Zh. Eksp. Teor. Fiz.* **53** 69 (Engl. Transl. 1991 *JETP Lett.* **53** 69)
[9] Hastings J B, Siddons D P, van Bürck U, Hollatz R and Bergmann U 1991 *Phys. Rev. Lett.* **66** 770
[10] Monahan J E and Perlow G J 1979 *Phys. Rev.* A **20** 1499
[11] Perlow G J, Monahan J E and Potzel W 1980 *J. Physique Coll.* **41** C1 85
[12] Helisto P, Ikonen E, Katila T and Riski K 1982 *Phys. Rev. Lett.* **49** 1209
Ikonen E, Helisto P, Katila T and Riski K 1989 *Phys. Rev.* A **32** 2298
[13] Helisto P, Tittonen I, Lippmaa M and Katila T 1991 *Phys. Rev. Lett.* **66** 2037
[14] Shvyd'ko Yu V, Smirnov G V and Popov S L 1991 *Pis. Zh. Eksp. Teor. Fiz.* **53** 217 (Engl. Transl. 1991 *JETP Lett.* **53** 231)
[15] Asher J, Cranshaw T E and O'Connor D A 1974 *J. Phys. A: Math., Nucl. Gen.* 7 410
[16] Tsankov L T 1981 *J. Phys. A: Math. Gen.* **14** 275
[17] Popov S L, Smirnov G V and Shvyd'ko Yu V 1989 *Pis. Zh. Eksp. Teor. Fiz.* **49** 651 (1989 *JETP Lett.* **49** 747)
Popov S L, Smirnov G V and Shvyd'ko Yu V 1990 *Hyperfine Interact.* **58** 2463
[18] Ruby S L and Bolef D I 1960 *Phys. Rev. Lett.* **5** 5
[19] Cranshaw T E and Reivari P 1967 *Proc. Phys. Soc.* **90** 1059
[20] Mitin A V 1976 *Sov. Quantum Electron.* **3** 840
[21] Dzyublik A Yu 1984 *Phys. Status Solidi* b **123** 53; 1986 *Phys. Status Solidi* b **134** 503
[22] Tsankov L T 1980 *J. Phys. A: Math. Gen.* **13** 2959, 2969
[23] Allen L and Eberly J H 1975 *Optical Resonance and Two-Level Atoms* (New York: Wiley) part I, section 6
[24] Hannon J P and Trammell G T 1989 *Physica* B **159** 161
[25] Mkrtchyan A R, Aturyunyan G A, Arakelyan A R and Gabrielyan R G 1979 *Phys. Status Solidi* b **92** 23